Experimental and theoretical study of the electronic structure of $AuAl_2$, $AuGa_2$, and $AuIn_2$

Li-Shing Hsu
Department of Physics, National Chang-Hua University of Education, Chang-Hua 50058, Taiwan, Republic of China

Y.-K. Wang
Center for General Education, Tajen Institute of Technology, Pingtung 907, Taiwan, Republic of China

Y.-L. Tai and J.-F. Lee
National Synchrotron Radiation Research Center, Hsinchu 30077, Taiwan, Republic of China

(Received 30 December 2004; revised manuscript received 21 July 2005; published 19 September 2005)

The binding energies of the Au 5*d* bands at the Γ point for $AuAl_2$, $AuGa_2$, and $AuIn_2$ calculated from the first-principles theory agree with those obtained from the angle-integrated or angle-resolved photoemission spectroscopic study to within 10%. X-ray absorption near-edge spectroscopy (XANES) spectra of these three compounds are presented and compared with theoretical XANES spectra and site- and momentum-decomposed partial density of states. Extended x-ray absorption fine structure spectra of $AuAl_2$, $AuGa_2$, and $AuIn_2$ are also analyzed to yield the bonding parameters.

DOI: 10.1103/PhysRevB.72.115115 PACS number(s): 78.70.Dm, 78.20.Ls, 75.50.Cc

I. INTRODUCTION

The present study is to use x-ray absorption near-edge spectroscopy (XANES), extended x-ray absorption fine structure (EXAFS) spectroscopy, and first-principles theoretical calculation to study the electronic structures of three interesting materials: $AuAl_2$, $AuGa_2$, and $AuIn_2$. These intermetallic compounds, which all crystallize in the cubic fluorite (CaF_2) structure, exhibit anomalies in various physical properties.[1,2] The discovery of the coexistence of the nuclear ferromagnetism and superconductivity in $AuIn_2$ attracts more interest.[3] It is noted that the total density of states (DOS) of these three compounds calculated by the relativistic parameter-based method[4] showed three Au 5*d* bands (Γ_8^1, Γ_7, and Γ_8^2), and the middle Γ_7 band was resolved in the later synchrotron-radiation-excited angle-integrated[5] and angle-resolved[6,7] photoemission spectroscopic (ARPES) studies. The crystal-field and spin-orbit parameters were then determined for $AuAl_2$, $AuGa_2$, and $AuIn_2$. In contrast to the above studies, the Γ_7 band of $AuAl_2$ was not resolved by previous angle-integrated photoemission study;[5] while that of $AuIn_2$ was not resolved by any of the previous x-ray photoemission spectroscopic studies.[8–11] This means that higher energy resolution is needed to study in detail the Au 5*d* valence bands of these compounds. To our knowledge, there are only a few papers[12,13] published on the Au $L_{2,3}$ XANES spectra of these three compounds. The purpose of this work is to study, both experimentally and theoretically, XANES and EXAFS spectra around Au L_3, Ga *K*, and In L_3 and *K* absorption edges in order to probe the angular-momentum-resolved unoccupied states and bonding properties of these three intermetallic compounds.

II. EXPERIMENT AND THEORY

Preparation of the single-crystal $AuAl_2$, $AuGa_2$, and $AuIn_2$ samples was reported previously.[5,6] X-ray absorption spectra of these three intermetallics were recorded at beamline 17C1 (for Au *L* and Ga *K* edges), beamline 01C1 (for In *K* edge), and beamline 15B1 (for In *L* edge) of the National Synchrotron Radiation Research Center, Taiwan. The samples were measured at room temperature in the fluorescence mode with normal-incidence and grazing-exit geometry in order to eliminate the self-absorption effect.[14] An appropriate filter (Ga and As filter for the Au L_3 and Au L_2 edge, respectively, Zn filter for the Ga *K* edge, and Ag filter for the In *K* edge) along with a set of Soller slits were placed between the sample and the detector to keep the background level as low as possible. For the In *L* edge, no filter was used. The energy resolution for the Au L_3, Ga *K*, In L_3, and In *K* level is 0.6, 0.5, 0.2, and 1.4 eV, respectively. Standard Au and In foils and GaO powder were used as references for energy calibration. The photon flux was obtained simultaneously by measuring the current of a Au mesh located near the exit slit of the Si(111) double-crystal monochromator and used for the normalization of the respective XANES and EXAFS spectra.

Analysis of the EXAFS spectra of these three compounds was carried out by using the UWXAFS 3.0 software package.[15] The fitting was corrected for the self-absorption effect first, but the difference in fitting quality with no correction for this effect is small. Curve-fitting procedures began with the *ab initio* calculation of the phase-shift and backscattering amplitude functions for single scattering of atom pairs using the FEFF6 code.[15] The fitting was made in the *r* space within the range of the specific peak. For a good fit, the goodness-of-fit parameter[16] was always below 0.02.

The theoretical XANES spectra of $AuAl_2$, $AuGa_2$, and $AuIn_2$ are calculated relativistically using the highly accurate all-electron full-potential linear augmented-plane-wave method (FLAPW).[17] The four-component (including *s*, *p*, *d*, and *f* orbitals) version of the WIEN2K code was used in the spin-orbit calculation.[17] The calculations are based on first-principles density functional theory with the generalized gradient approximation (GGA) to the exchange-correlation

TABLE I. The theoretical and experimental lattice constant (a), bulk modulus (B), and total DOS at $E_F[n(E_F)]$ of $AuAl_2$, $AuGa_2$, and $AuIn_2$.

Material	Method	a (Å)	B (Mbar)	$n(E_F)$ (states/eV cell)
$AuAl_2$	LDA	5.97	1.19	0.93
	GGA	6.07	1.03	0.92
	Exp.	6.0[a]		1.28[b]
$AuGa_2$	LDA	6.03	0.96	0.92
	GGA	6.22	0.69	0.90
	Exp.	6.08[a]		1.14[b]
$AuIn_2$	LDA	6.47	0.79	1.02
	GGA	6.68	0.54	1.02
	Exp.	6.51[a]		1.33[b]

[a]Reference 1.
[b]Reference 22.

potential.[18] The calculations were also repeated within the local density approximation (LDA) to estimate the sensitivity of the results to the exchange correlation potential used. We begin the calculation by determining total energies at 11 values of the lattice constant near the experimental ones. These energies are then fitted to the Murnaghan equation of state[19] to obtain the theoretical equilibrium lattice constants and bulk moduli, which are listed in the third and fourth columns, respectively, in Table I. The relativistic effects reduce the difference between the calculated and measured lattice constants of these compounds. We noted that the theoretical lattice constants of these three compounds calculated by the LDA approximation agree better with the experimental values than those calculated by the GGA method. The same observation was found for $PtGa_2$.[20] In Table I, the GGA overestimates the lattice parameters of $AuAl_2$, $AuGa_2$, and $AuIn_2$ by 1.2%, 2.3%, and 2.6%, respectively. Furthermore, the LDA is known to describe the Au lattice better than does the GGA.[21] Thus, we used the LDA in the rest of this paper. The core state is chosen as [Xe], [Ne], [Ar], and [Kr] for Au, Al, Ga, and In atoms, respectively. The muffin-tin radius of 1.43, 1.16, 1.16, and 1.32 Å is used for Au, Al, Ga, and In atoms, respectively. The wave functions, the charge densities, and the potentials are expanded in terms of the spherical harmonics inside the muffin-tin spheres. The cutoff angular momentum ($l_{\max}$) of 10 used for the wave functions and six used for the charge densities and the potentials are sufficient for accurate total-energy calculations.[17] However, we also did a complete cycle of self-consistent field (SCF) calculations for $l_{\max}=8$, and indeed, the thus calculated total energy, DOS, and XANES spectra are essentially the same as those obtained for $l_{\max}=6$. The Brillouin zone (BZ) integration is carried out by using the improved tetrahedron method.[22] The number of the augmented plane waves included is about 135 per atom, i.e., $R_{\mathrm{mt}}K_{\max}=9$. In the calculation of theoretical equilibrium lattice constants, the number of the k points used in the irreducible BZ wedge (IBZW) is 72. In the final calculation, a larger number of 256 k points in the IBZW and the experimental lattice constants were used in the self-consistent total-energy calculations. Since our theoretical equilibrium lattice constants are close to the experimental ones, using either value is not expected to have a significant effect on the calculated XANES spectra and DOS curves. Additionally, we used an even larger number of k points (680) in the IBZW to do a complete cycle of full SCF calculations. The minimum of the total energy is shifted upward only by 0.37, 0.78, and 0.67 meV for $AuAl_2$, $AuGa_2$, and $AuIn_2$, respectively, by the transition from 256 to 680 k points with $l_{\max}=6$. The DOS and XANES spectra are essentially the same as those calculated using 256 k points.

III. RESULTS AND DISCUSSION

A. Valence-band parameters of $AuAl_2$, $AuGa_2$, and $AuIn_2$ and the total DOS values

The angle-integrated photoemission spectra of $AuAl_2$ and $AuIn_2$ were published previously.[5] The only ARPES spectra of $AuAl_2$ was reported by Hsu *et al.*,[7] and those of $AuGa_2$ and $AuIn_2$ were reported by Nelson *et al.*[6] In Table II, the experimental and theoretical binding energies (E_B) of the Au $5d$ bands at Γ_8^1, Γ_7, and Γ_8^2 for $AuAl_2$, $AuGa_2$, and $AuIn_2$ derived from the above three photoemission measurements and present FLAPW calculations including the spin-orbit coupling are listed. The most important relativistic effect is the splitting of the Γ_{25} states into Γ_7 and Γ_8 states as shown in Table II. We note that the theoretical E_B values at the three Γ points calculated with the LDA and GGA are essentially the same. We should also point out that these theoretical E_B values are within 10% from the experimental ARPES ones, except for that at the Γ_8^1 point of $AuAl_2$ (with a 14.7% difference). The value of the total DOS at the Fermi energy (E_F) $[n(E_F)]$ for $AuAl_2$, $AuGa_2$, and $AuIn_2$ calculated by using the LDA is 0.93, 0.92, and 1.02 states/eV cell, respectively, as shown in the last column in Table I. We note that those values calculated by using the GGA are essentially the same as these, and both approximations underestimate the experimental total DOS. These $n(E_F)$ values are comparable, respectively, to those calculated by using the parameter-based method[1] (1.08, 1.12, and 1.02 states/eV cell) and to the values[23] (1.28, 1.14, and 1.33 states/eV cell) derived from the specific-heat measurement. The experimental $n(E_F)$

TABLE II. The experimental and theoretical binding energies of the Au 5*d* bands at the Γ point for $AuAl_2$, $AuGa_2$, and $AuIn_2$. All values in eV and referred to the Fermi energy.

	E_B (Γ_8^1)	E_B (Γ_7)	E_B (Γ_8^2)	Reference
$AuAl_2$	5.05		6.95	5[a]
	4.90	5.80	6.85	7[b]
	5.62	6.33	6.98	This work[c]
	5.61	6.31	7.0	This work[d]
$AuGa_2$	4.92	5.68	7.31	6[b]
	5.16	5.95	7.28	This work[c]
	5.23	5.99	7.27	This work[d]
$AuIn_2$	4.75	5.45	6.50	5[a]
	4.72	5.48	7.05	6[b]
	4.88	5.37	6.46	This work[c]
	4.94	5.43	6.46	This work[d]

[a]Angle-integrated photoemission study.
[b]ARPES study.
[c]LDA.
[d]GGA.

values obtained from the specific-heat measurement are the theoretical $n(E_F)$ values enhanced by a factor $1+\lambda$, where λ is the electron-phonon mass enhancement parameter. The λ value thus determined for $AuAl_2$, $AuGa_2$, and $AuIn_2$ is 0.38, 0.25, and 0.30, respectively. We note that the λ value for $PtGa_2$ is 0.45.[20] This observation explains in part why $PtGa_2$ has the highest superconducting transition temperature[1] (2.15 K) among these four intermetallics.

B. XANES spectra of $AuAl_2$, $AuGa_2$, and $AuIn_2$ and the partial DOS curves

The experimental (open circles) and theoretical (solid line) Au L_3-edge XANES spectra for $AuAl_2$, $AuGa_2$, and $AuIn_2$ are displayed in Figs. 1(a)–1(c), respectively. The corresponding Ga *K*-edge and In L_3- and *K*-edge XANES spectra for $AuGa_2$ and $AuIn_2$ are displayed in Fig. 2 and Figs. 3(a) and 3(b), respectively. These theoretical XANES spectra were calculated by the WIEN2K program.[17] We note that the calculated XANES spectra are essentially the same as those calculated without the spin-orbit coupling within plotting accuracy. The theoretical XANES spectra have been broadened with a Lorentzian of full width at half maximum of 3 eV to simulate the broadening due to both instrument and core-hole lifetime. According to the dipole-transition selection rule, the Au L_3, Ga *K*, and In L_3 and *K* white-line features correspond, respectively, to the transitions from Au $2p_{3/2}$ to $5d_{5/2}$, Ga 1*s* to 2*p*, In $2p_{3/2}$ to $4d_{5/2}$, and In 1*s* to 2*p* states. Thus, also plotted in these figures are the Au $s+d$, Ga *p*, In $s+d$, and In *p* angular-momentum-decomposed partial DOS curves (dashed lines) calculated for these intermetallic compounds. The maximum of each XANES spectrum coincides with the peak in the corresponding partial DOS curve. The zero energy corresponds to the inflection point of the Au L_3-, Ga *K*-, In L_3-, and In *K*-edge absorption thresholds of 11 919, 10 367, 3730, and 27 940 eV, respectively. Overall, we have

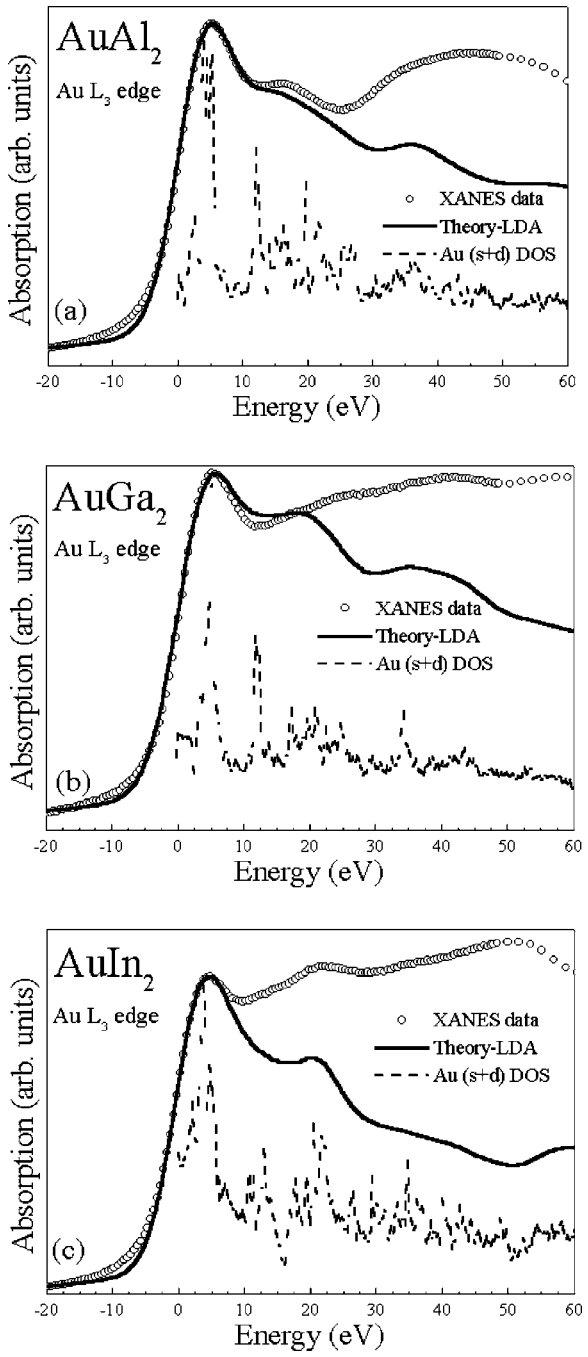

FIG. 1. The Au L_3-edge XANES spectra for (a) $AuAl_2$, (b) $AuGa_2$, and (c) $AuIn_2$.

a reasonably good agreement between theory and experiment. All major features of the absorption peaks, as well as white-line positions and intensities, are well reproduced. For example, the energies (with respective to the energy of the inflection point) of the peaks of the Ga *K*-edge experimental XANES spectrum for $AuGa_2$ are 6.5, 14.5, 32.5, and 44.3 eV; while the corresponding theoretical values are 6.8, 14.6, 29.8, and 45.6 eV. The worst agreement between theory and experiment is found for the In L_3 edge of $AuIn_2$. The theoretical Au L_3-edge XANES spectra for these compounds were calculated by including higher-energy (up to 10 eV above E_F) unoccupied Au *s* and *d* states to improve

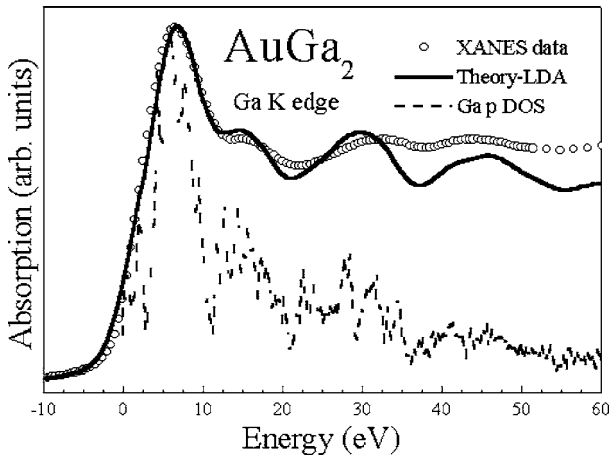

FIG. 2. The Ga *K*-edge XANES spectra for $AuGa_2$.

the agreement in intensity with experimental spectra. The improvement is least for the Au L_3 edge of $AuIn_2$. The decrease in intensity after the second peak of the theoretical Au L_3-edge XANES spectra for $AuAl_2$ and $AuGa_2$ is due to the finite-sized, linearized energy-dependent basis sets in the muffin-tin spheres used in the present calculations. This disagreement could be further improved by including more orbitals inside the Au muffin-tin sphere, but it is not the main concern in this paper.

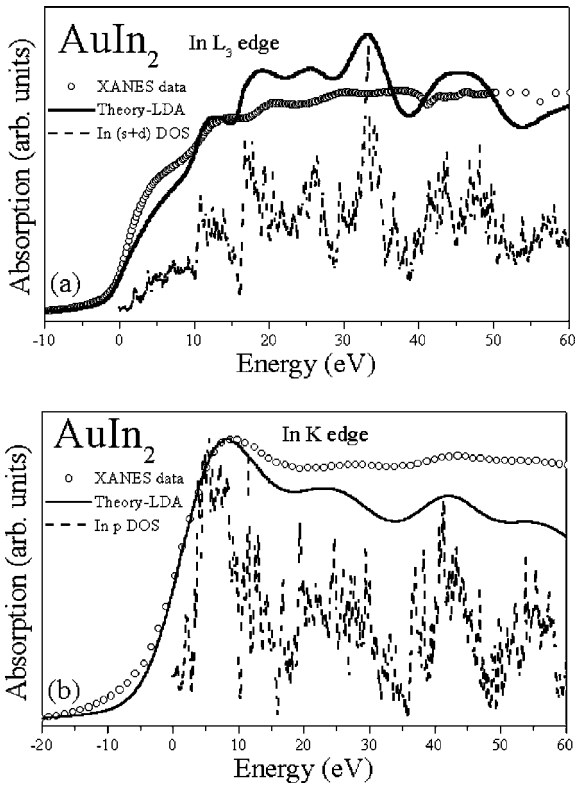

FIG. 3. The In (a) L_3-edge and (b) *K*-edge XANES spectra for $AuIn_2$.

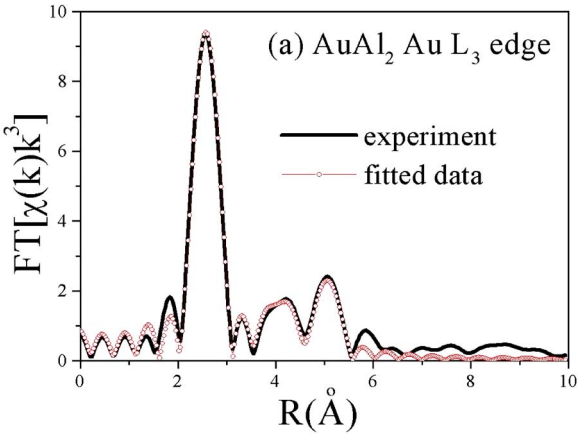

FIG. 4. (Color online) The experimental (solid lines) and the theoretical fitted (open circles) Fourier transforms of k^3-weighted Au L_3-edge EXAFS spectra for $AuAl_2$.

C. EXAFS spectra of $AuAl_2$, $AuGa_2$, and $AuIn_2$ and the bonding parameters

Figure 4 shows the experimental (solid lines) and the theoretically fitted (open circles) Fourier transforms of k^3-weighted Au L_3-edge EXAFS spectra for $AuAl_2$. Similar spectra were obtained for Au metal, $AuGa_2$, and $AuIn_2$. These theoretical fitting of the EXAFS spectra were performed by using the UWXAFS 3.0 software package.[15] The bond distance (R), the coordination number (N), and the scaling constant (σ^2) for the first and second shells around Au or Ga (In) atoms for Au foil, $AuAl_2$, $AuGa_2$, and $AuIn_2$ derived from the Au L_3- or Ga (In) *K*-edge EXAFS spectra are listed in the third, fourth, and fifth columns, respectively, in Table III. In the fitting the ratio of N's for different shells was fixed to the crystallographic values since the N value is highly correlated with the Debye-Waller factor. The calculated Au—Au bond length for Au foil is 2.87 Å, which is exactly the same as the bulk value. The calculated Au—Al and the Au—Au bond length for $AuAl_2$ is 2.58 and 4.21 Å,

TABLE III. The bond distance (R), the coordination number (N), and the scaling constant (σ^2) for the first and second shells around Au or Ga (In) atoms derived from the Au L_3- or Ga (In) *K*-edge EXAFS spectra for Au foil, $AuAl_2$, $AuGa_2$, and $AuIn_2$.

Edge (material)	Shell	R (Å)	N	σ^2 (10^{-3} Å^2)
Au L_3 (Au foil)	Au—Au	2.87	8.6	6.6
Au L_3 ($AuAl_2$)	Au—Al	2.58	7.3	6.3
	Au—Au	4.21	10.9	10.9
Au L_3 ($AuGa_2$)	Au—Ga	2.60	6.2	5.9
	Au—Au	4.33	9.4	13.4
Ga K ($AuGa_2$)	Ga—Au	2.59	2.3	2.7
	Ga—Ga	3.00	3.5	9.8
Au L_3 ($AuIn_2$)	Au—In	2.79	5.4	6.2
	Au—Au	4.52	8.1	20.6
In K ($AuIn_2$)	In—Au	2.81	3.3	6.4
	In—In	3.23	5.1	13.9

respectively, which is very close to the corresponding bulk value of 2.60 and 4.24 Å. The calculated Au—Ga and the Ga—Au bond lengths for $AuGa_2$ are 2.60 and 2.59 Å, respectively, which are essentially the same as the bulk value of 2.63 Å; while the calculated Au—Au and the Ga—Ga bond lengths for $AuGa_2$ are 4.33 and 3.00 Å, respectively, which are very close to the respective bulk values of 4.30 and 3.04 Å. The calculated Au—In and In—Au bond lengths for $AuIn_2$ are 2.79 and 2.81 Å, respectively, which are essentially the same as the bulk value of 2.82 Å; while the calculated Au—Au and In—In bond lengths for $AuIn_2$ are 4.52 and 3.23 Å, respectively, which are very close to the respective bulk values of 4.60 and 3.26 Å. However, the agreement between the N values and those expected from simple crystal-structure calculation is much worse. For example, in $AuGa_2$ the Au atom has eight nearest-neighbor Ga atoms, and 12 second-nearest-neighbor Au atoms; while the Ga atom has four nearest-neighbor Au atoms, and six second-nearest-neighbor Ga atoms. The corresponding value obtained from the EXAFS analysis is 6.2, 9.4, 2.3, and 3.5, respectively. This is because the N values contain much more uncertainty than the R values in the EXAFS analysis. From Table III, one can see that the σ^2 value for the second shell is much larger than that of the first shell, with the largest value (20.6) occurring for the Au L_3 edge of $AuIn_2$.

IV. CONCLUSIONS

The calculated binding energies at the Γ point of the Au $5d$ bands for $AuAl_2$, $AuGa_2$, and $AuIn_2$ agree with those obtained from the angle-integrated or angle-resolved photoemission spectroscopic studies to within 10%. The theoretical total DOS's of these materials are compared with the experimentally derived values. Experimental Au L_3-, Ga K-, and In L_3- and K-edge XANES spectra of these three compounds are compared with theoretical XANES spectra and site- and momentum-decomposed partial DOS curves. Au L_3-, Ga K-, and In K-edge EXAFS spectra of these three intermetallics are analyzed to yield their structural and bonding parameters.

ACKNOWLEDGMENTS

We thank G. Y. Guo for calculation assistance and acknowledge support from the National Science Council, Taiwan.

[1] L.-S. Hsu, Mod. Phys. Lett. B **8**, 1297 (1994), and references therein.
[2] B. K. Godwal, S. Meenakshi, P. Modak, R. S. Rao, S. K. Sikka, V. Vijayakumar, E. Bussetto, and A. Lausi, Phys. Rev. B **65**, 140101(R) (2002), and references therein.
[3] S. Rehmann, T. Herrmannsdorfer, and F. Pobell, Phys. Rev. Lett. **78**, 1122 (1997).
[4] S. Kim, J. G. Nelson, and R. S. Williams, Phys. Rev. B **31**, 3460 (1985).
[5] L.-S. Hsu, H.-W. Huang, and K.-L. Tsang, J. Phys. Chem. Solids **59**, 1205 (1998).
[6] J. G. Nelson, W. J. Gignac, S. Kim, J. R. Lince, and R. S. Williams, Phys. Rev. B **31**, 3469 (1985).
[7] L.-S. Hsu, G. Y. Guo, J. D. Denlinger, and J. W. Allen, J. Phys. Chem. Solids **62**, 1047 (2001).
[8] S. Hufner, J. H. Wernick, and K. W. West, Solid State Commun. **10**, 1013 (1972).
[9] T. K. Sham, M. L. Perlman, and R. E. Watson, Phys. Rev. B **19**, 539 (1979).
[10] P. M. Th. M. van Attekum, G. K. Wertheim, G. Crecelius, and J. H. Wernick, Phys. Rev. B **22**, 3998 (1980).
[11] H.-G. Boyen, R. Gampp, P. Oelhafen, B. Heinz, P. Ziemann, Ch. Lauinger, and St. Herminghaus, Phys. Rev. B **56**, 6502 (1997).
[12] A. Bzowski, Y. M. Yiu, and T. K. Sham, Phys. Rev. B **51**, 9515 (1995).
[13] T. K. Sham, Solid State Commun. **64**, 1103 (1987).
[14] L. Troger, D. Arvanitis, K. Baberschke, H. Michaelis, U. Grimm, and E. Zschech, Phys. Rev. B **46**, 3283 (1992).
[15] E. A. Stern, M. Newville, B. Ravel, and D. Haskel, Physica B **208–209**, 117 (1995).
[16] J. J. Rehr, J. M. de Leon, S. I. Zabinsky, and R. C. Alberts, J. Am. Chem. Soc. **113**, 5135 (1991).
[17] P. Blaha, K. Schwarz, G. K. H. Madsen, D. Kvasnicka, and J. Luitz, computer code WIEN2K (K. Schwarz, Techn. University Wien, Austria, 2001).
[18] J. P. Perdew, K. Burke, and M. Ernzerhof, Phys. Rev. Lett. **77**, 3865 (1996).
[19] F. D. Murnaghan, Proc. Natl. Acad. Sci. U.S.A. **3**, 244 (1944).
[20] L.-S. Hsu, G. Y. Guo, J. D. Denlinger, and J. W. Allen, Phys. Rev. B **63**, 155105 (2001).
[21] Z. Yang, R. Wu, Q. Zhang, and D. W. Goodman, Phys. Rev. B **65**, 155407 (2002).
[22] P. E. Blöchl, O. Jepsen, and O. K. Andersen, Phys. Rev. B **49**, 16223 (1994).
[23] J. A. Rayne, Phys. Lett. **7**, 114 (1963).